

The method of multiple sampling by significance for the visualization of functionally defined scenes

Sergey Vyatkin^{1*} and Boris Dolgovesov¹

¹Institute of Automation and Electrometry SB RAS, acad. Koptuga, 1, 630090 Novosibirsk, Russia

Abstract. In ray tracing methods, the key point is to choose the direction for the rays. If many rays are needed not everywhere, but only in some parts of the scene, it is reasonable to increase the selection in these places. As a result, computing resources are not wasted where there is no such need. That is, you need to make selections by significance. In this paper, the visualization of functionally defined scenes is considered. A method of multiple sampling by significance is proposed. The method uses weight functions for multiple sampling by significance. The weighting functions minimize the variance of the multiple sample estimation by significance. Weights can be negative, which reduces the variance. In addition, weights allow you to have additional flexibility when developing a sampling method that accelerates calculations. As a result, acceptable weights were obtained when modeling light transfer. The variance was reduced by using weights in the sample. The dependence of the mean square error on the number of samples is given. Highly realistic functionally defined scenes are visualized. The method is implemented using CPU and GPU. Diagrams of the method's performance are given. Keywords: ray tracing, functionally defined scene, weighing functions, environment sampling, multiple sampling by significance

1 Introduction

The following methods of sampling by significance are known. The environment sample includes ambient lighting and a light dome. Multiple significance sampling is used for both light and materials with a balance between them. Extended multiple sampling by significance is used for realistic rendering of materials such as leather, marble, wax, etc. The Monte Carlo method is often used to simulate light transport [1, 2]. However, the Monte Carlo method is characterized by slow convergence. To reduce the variance, methods of sampling by significance were proposed, as well as their extension-multiple sampling by significance [3, 4]. Multiple significance sampling is used in bidirectional path sampling methods [5, 6], adaptive path sampling methods [7], modern path tracing methods for light transport [8], etc.

For the effectiveness of multiple sampling by significance, weight functions are used. The weight functions, known as the balance heuristic, give a smaller variance [9]. Alternative weights have also been proposed to address the disadvantages of the balance heuristic

*Corresponding author: sivser@mail.ru

variance. The application of different weighing methods depends on the specific task. Multiple significance sampling is used to mix bidirectional reflection distribution function and sampling methods. Multiple significance sampling is also used to select light transport paths [10]. The optimal target densities for the local direction of the path are described in [11]. In Monte Carlo Markov chain methods, multiple importance sampling is used to combine the contribution of the chains [12]. The distribution of samples based on the bidirectional distribution function of scattering, light, and photon maps is described in [13]. The method of the bi-directional reflection distribution function with oriented light sampling, which selects light sources based on importance values, is described in [14].

Standard methods of direct assessment of illumination consist in the random selection of light in accordance with the distribution of light. The light is selected in proportion to its actual contribution to the integral. However, this cannot be calculated analytically. Despite the fact that the light selection method may be close to ideal, an error in the estimation can significantly increase the variance or lead to bias.

In this paper, we propose weighting functions that minimize the variance of the estimation of a multiple sample of importance. Weights can be negative; this allows you to reduce the variance. The paper describes the weights of a multiple sample of importance. The o method is implemented, which provides significant acceleration. In the proposed method, the number of samples is set.

2 Method Description

Functionally defined surface is a composition of the basic function plus perturbations [15, 16]:

$$f'(x, y, z) = f(x, y, z) + \sum_{i=1}^n f_i r_i(x, y, z), \quad (1)$$

where r is the perturbation, f_i is the form factor,

$$r_i(x, y, z) = \begin{cases} q_i^3(x, y, z), & \text{if } q_i(x, y, z) \geq 0 \\ 0, & \text{if } q_i(x, y, z) < 0 \end{cases}, \quad (2)$$

where q is the perturbing function.

Multiple selection is determined by significance (an object with multiple selections) [3]:

$$F = \sum_{i=1}^m \sum_{j=1}^{n_i} \frac{\omega_i(v_{ij}) f(v_{ij})}{n_i d_i(v_{ij})}, \quad (3)$$

where v_{ij} is the j -th sample from n_i the samples, ω_i are the weight functions, m are the number of methods, d_i is the density.

The weight functions must satisfy the following conditions:

$$f(v) \neq 0 \Rightarrow \sum_{i=1}^m \omega_i(v) = 1, \quad (4)$$

$$d_i(v) = 0 \Rightarrow \omega_i(v) = 0, \quad (5)$$

Single-selection object:

$$F^1 = \frac{\omega_i(v_i)f(v_i)}{p_i d_i(v_i)}, \quad (6)$$

where p_i is the probability, v_i is the sample.

The strategy of the balance and power heuristics is described by the formula [10]:

$$\omega_i^p(v) = \frac{[n_i d_i(v)]^h}{\sum_{l=1}^m [n_l d_l(v)]^h}, \quad (7)$$

Using the balance and power heuristics, you can combine sampling methods. However, the overall efficiency decreases, because the combinations may be suboptimal.

If we consider models with multiple samples that allow negative weights, we can improve the variance.

We define a symmetric matrix $m \times m$ with elements given by

$$m_{il} = \frac{d_i, d_l}{\sum_{j=1}^m n_j d_j}, \quad (8)$$

The contribution vector is defined by:

$$\vec{c} = \frac{f, d_l}{\sum_{j=1}^m n_j d_j}, \quad (9)$$

The matrix is independent of the integrand f . It consists of the inner products between the probability densities (probability distribution functions) normalized by the coefficient $(\sum_{j=1}^m n_j d_j)^{-1}$. The elements of the contribution vector make up the contributions to the final one $F = \int_{v_{ij}} f(v) dv$. Since the dot product $(n_1, \dots, n_m) \cdot \vec{c}$ is equal to the integral F .

We write the initial estimate of $\langle F \rangle$ in the form:

$$\langle F \rangle^{cv} = \langle F \rangle + \sum_{i=1}^R \lambda_i (E_i - \langle E_i \rangle) = \sum_{i=1}^R \lambda_i E_i + \langle F \rangle - \sum_{i=1}^R \lambda_i \langle E_i \rangle, \quad n \quad (10)$$

Where R a set of estimators is $\langle E_i \rangle$, E_i are the expected values, $1, \dots, R$ is a set of random variables.

You can reduce the variance if $\langle E_i \rangle$ it correlates with $\langle F \rangle$. Vector $\vec{\lambda} = (\lambda_1, \dots, \lambda_R)^T$ is selected accordingly.

The variance is minimized to λ solve the system $\sum \lambda = \delta$. Where $\sum = \delta_{iR}$ is the covariance matrix $R \times R$. $\vec{\lambda} = (\lambda_1, \dots, \lambda_R)^T$ is the covariance vector.

The elements of the covariance vector are defined by:

$$\delta_{iR} = Cov[\langle E_i \rangle, \langle E_R \rangle], \delta_i = Cov[\langle E_i \rangle, \langle F \rangle] \quad (11)$$

Let the weighing function be expressed in the form (3)

$$\omega_i(v) = v_{ci} \frac{d_i(v)}{f(v)} + \frac{n_i d_i(v)}{\sum_{j=1}^m n_j d_j(v)} \left(1 - \frac{\sum_{j=1}^m v_{cj}(v)}{f(v)} \right), \quad (12)$$

We obtain an optimal estimate of the multiple optimal sample by the significance of $\langle F \rangle$ in the form:

$$\langle F \rangle^0 = \sum_{i=1}^m v_{ci} + \frac{1}{S} \sum_{i=1}^m \sum_{j=1}^{n_i} \left(\frac{f(v_{ij})}{\eta(v_{ij})} - \frac{\sum_{R=1}^m v_{cR} d_R(v_{ij})}{\eta(v_{ij})} \right), \quad (13)$$

where $S = \sum_{i=1}^m n_i$, $\eta = \sum_{i=1}^m \rho_i d_i(v)$, $\rho = n_i / S$.

Using the vector \vec{v}_c , we obtain the optimal control variation (13), with minimizing its variance. The variance is equal to the variance of the balance heuristic estimate.

The more the form of the function and the integrand coincide, the smaller the variance. Because of the optimal weights compared to the balance heuristic. The variance $\langle F \rangle$ becomes zero when the integrand can be written as a linear combination of sample files. The variance of the optimal estimate is less than or equal to the heuristic variance of the balance. The balance heuristic is optimal when the elements of the vector \vec{v}_c are proportional to the number of samples from the individual sampling methods. This is used to improve the variance over the balance heuristic.

Since the inner products forming the matrix of the method and the contribution vector do not have a closed-form solution, the multiple-sample significance estimate with optimal weights cannot be determined directly. The elements of the method matrix and the contribution vector are given by integrals. These integrals are first evaluated, using multiple significance sampling with a balance heuristic. The vector \vec{v}_c is given by a linear system. It is then \vec{v}_c evaluated using the least squares minimization method. The resulting multiple-sample significance score will be true for any value \vec{v}_c .

You can apply various options for approximating the optimal estimate of $\langle F \rangle$. For example, you can estimate \vec{v}_c from the initial batch of samples. Then fix it and use it to estimate the optimal weights for all subsequent samples. However, this approach is not optimal, since the assumed ones \vec{v}_c will not evolve over time. A more effective method is to gradually implement an approximate estimate.

The calculation is performed in iterations. At each iteration, we display samples n_i from each sampling method $d_i, i = 1, \dots, m$. Then we calculate the vector \vec{v}_c based on the estimates from the previous iterations. We include the vector in formula (13) to calculate the integral estimate for the current samples and accumulate it. For the first iteration, we set the vector \vec{v}_c to zero. The form and parameters of the optimal estimate (13) are obtained by directly minimizing the variance of the multiple-sample estimate by significance.

Figure 1 shows the basic steps of calculations. First, a beam is emitted from the camera or light source, the beam is tracked. If there is no intersection, then the process ends and the algorithm proceeds to the next selection. Otherwise, the algorithm processes the surface radiation, if any. Then, if an assessment of the next event is required, a new shadow ray is emitted to the light source. At the end, either the algorithm generates a continuation beam, or the process terminates.

When rendering objects, materials are presented with an appropriate bidirectional scattering distribution function. This function is used in combination with the visualization equation to calculate the light scattering on the surface. The algorithm uses multiple sampling by importance. It is also possible to query the sampling probability for a given direction.

Light sources are located separately from the surfaces of objects. Light sources may not have a specific area and may be processed in different ways. This applies, for example, to point light sources. The selection, determination of the position and direction of the light source is carried out. Shaders generate materials with a combination of texture, bidirectional scattering distribution function and light sources.

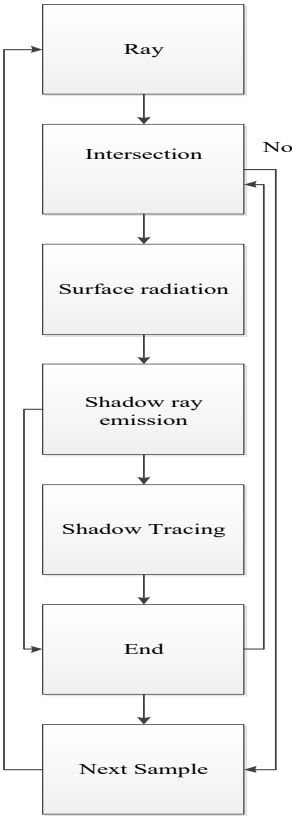


Fig. 1. Rendering algorithm.

3 Results

The method was tested using two approaches. The uncorrelated version uses two independent sets of samples to estimate the method matrix and the contribution vector. The correlated version uses a single set of samples to estimate the method matrix and contribution vector.

The behavior of the function in the uncorrelated case is very different, since both estimates perform much worse than in the correlated case. The correlation between the estimates of the method matrix and the contribution vector improves the performance of both estimators.

Both the shape and the mixing parameters \vec{v}_c for the estimate are obtained by directly minimizing the variance of the multiple-sample estimate by significance. It also provides an optimal solution.

The method can be used for alternative strategies for approximating the optimal matrix of the method, the contribution vector, and \vec{v}_c .

Evaluating and solving a linear system leads to computational overhead. The computational overhead increases linearly with the number of combined methods. On the other hand, the overhead in our tests was almost negligible, especially for the direct estimator. However, they increase as the number of sampling methods increases.

The scenes are rendered on a machine with a Core i7-4790K processor (4 cores, 8 threads) and GPU GTX 980. Direct estimates are implemented; calculations are performed pixel by pixel. The algorithm is started, and the output data is stored in a pixel. One sample is taken for each iteration.

Figure 2, on the left, shows the results in a scene illuminated by multiple light sources of a small area. Images using optimal weights were rendered using the same number of samples per pixel (thirty samples).

A single large light from above illuminates the stage (Figure 2, right). The images were rendered using direct estimation, the number of samples per pixel (forty samples). The combination with a uniform area reduces the dispersion mainly on the table; the combination with optimal weights improves the result on surfaces that are not parallel to the light (for example, on the sidewalls of the table).



Fig. 2. Left: a scene with multiple light sources; right: the scene is rendered with an increase in the number of samples per pixel (forty samples).

The behavior of optimal weights for a combination of light-domain sampling methods and a bidirectional scattering distribution function is investigated. The illumination from individual light sources is evaluated separately. By combining the illumination area and sampling the bidirectional scattering distribution function, we add the contributions together. Figure 3 shows a graph of the dependence of the root-mean-square error on the number of iterations, built on a logarithmic scale.

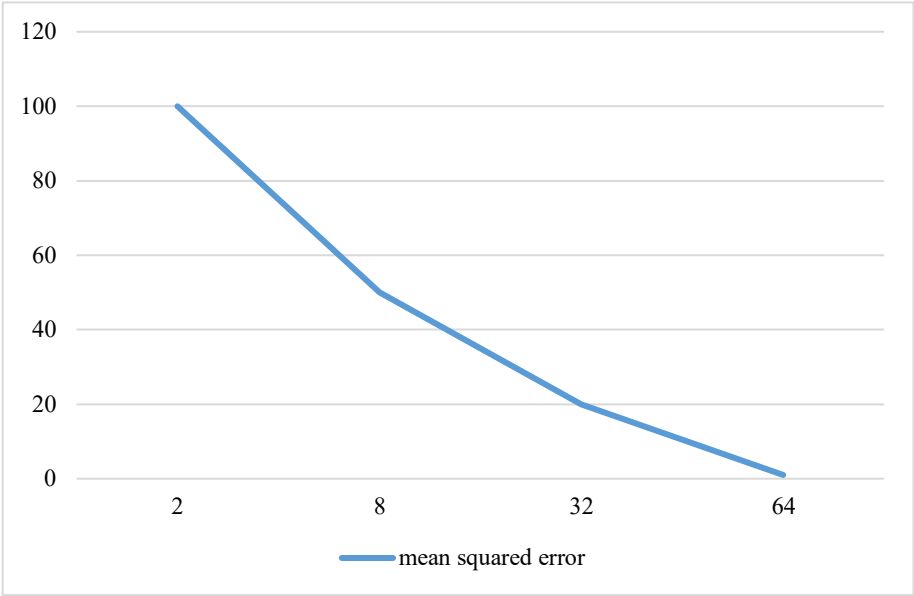


Fig. 3. Dependence of the mean square error on the number of samples.

The root-mean-square error is a metric that is used to evaluate the effectiveness of the model. To calculate it, the number of detected errors is squared and the average value is calculated.

Table 1 shows Speed Up, Improvement and Overhead.

Speed Up and Improvement are the relations of the root-mean-square error. Overhead is a relative increase in rendering time with the same total number of samples.

Table 1. Method performance statistics.

Scenes	Speed Up	Improvement	Overhead
Fig. 2 Left	8.9	9.5	9.7%
Fig. 2 Right	9.4	10.03	5.8%

Figure 4 shows the average distribution of scene calculation time on Core i7-4790K. The time is measured with tracking of the camera, secondary and shadow rays with shading. In addition, the generation, sorting and compaction of beams are taken into account. The ordinate axis shows the time in milliseconds.

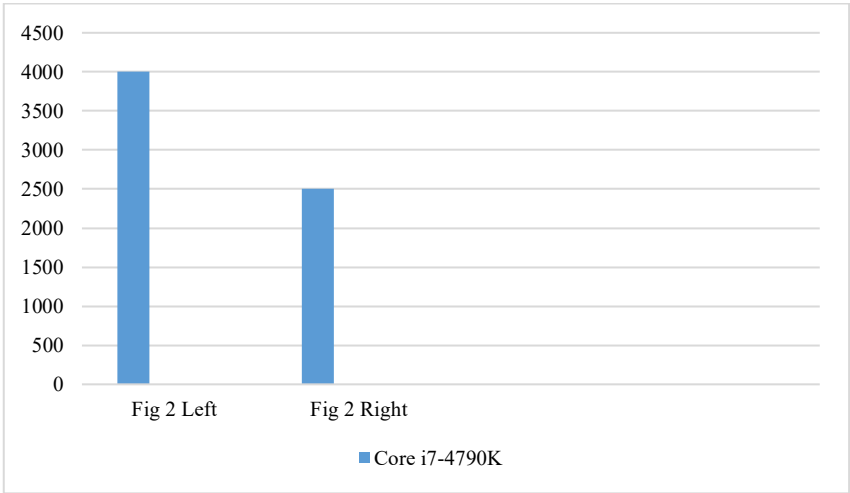


Fig. 4. Average scene calculation time on Core i7-4790K.

Figure 5 shows the performance of the Core i7-4790K GPU and GTX 980. The ordinate axis shows the number of MRays/s.

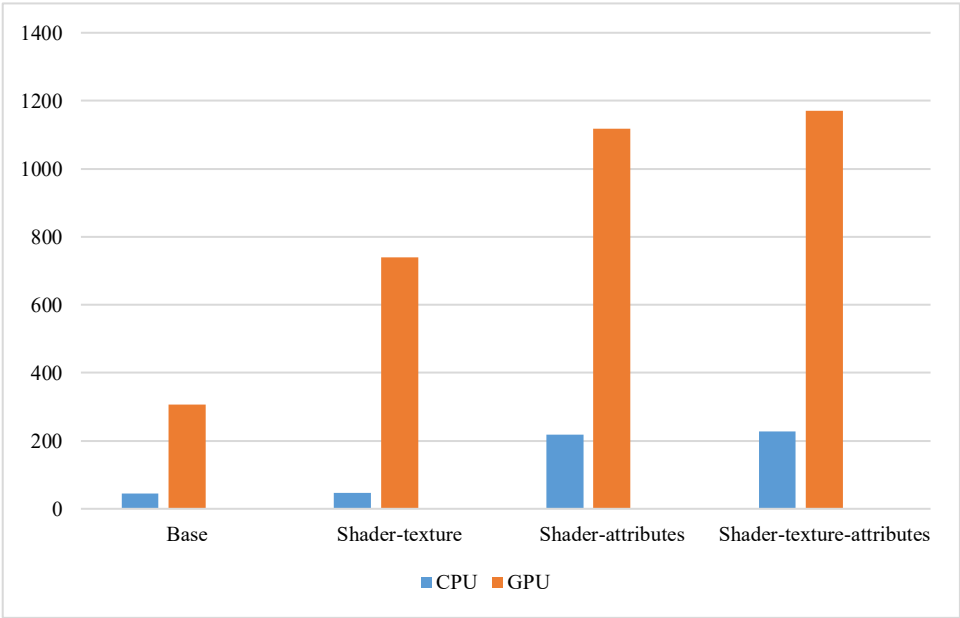


Fig. 5. Performance of Core i7-4790K GPU and GTX 980 in MRays/s.

Table 2. Shows a comparison of performance in MSamples/s for CPU and GPU for different scenes.

Table 2. Performance in MSamples/s.

Scenes	CPU	GPU
Fig 2 Left	9.7	41.3
Fig 2 Right	6.5	29.5

4 Conclusion

The method of multiple significance sampling is presented. The paper also uses negative weight functions, which expands the class of effective combinational strategies.

Weights are relevant for a sample where the balance heuristic is inefficient. The dispersion properties of the optimal weights give additional positive qualities. The proposed method is aimed at improving the effectiveness of combined assessments.

References

1. A. Gruson, B. S. Hua, T. Hachisuka, G. Singh, *ACM trans graphics* **41**(4), 1-14 (2022) <https://doi.org/10.1145/3528223.3530095>
2. J. Beck, Y. Liu, E. V. Schwerin, R. Tempone, *Computer Methods in Applied Mechanics and Engineering* **402** (2022) <https://doi.org/10.1016/j.cma.2022.115582>
3. V. Elvira, L. Martino, *Wiley Statistics Reference Online*, DOI:10.1002/9781118445112.stat08284
4. A. Lindqvist, *Ray Tracing Gems II*, DOI:10.1007/978-1-4842-7185-8_20
5. M.S. Nunes, F.M. Nascimento, G.F. Miranda, B.T. Andrade, Springer, *The Visual Computer* (2021) DOI:10.1007/s00371-020-02035-9
6. A. Wang, L. Ge, N. Holzschuch, *IEEE Transactions on Visualization and Computer Graphics* **99**, 1-1 (2019) DOI:10.1109/TVCG.2018.2890466
7. J.J. Guo, P. Bauszat, J. Bikker, E. Eisemann, *Computer Science* (2018) DOI:10.2312/sre.20181174
8. L. Fascione, J. Hanika, D. Heckenberg, C. Kulla, *ACM SIGGRAPH* (2019) DOI:10.1145/3305366.3328079
9. M. O. Berild, S. Martino, V. G. Rubio, H. Rue, *Journal of Computational and Graphical Statistics* **31**(4), 1-25 (2022) DOI:10.1080/10618600.2022.2067551
10. P. Grittmann, O. Yazici, I. Georgiev, P. Slusallek, *ACM Transactions on Graphics* **41**(4), 1-12 (2022) DOI:10.1145/3528223.3530126
11. A. Rath, P. Grittmann, S. Herholz, *ACM Transactions on Graphics* **39**(4) (2020) DOI:10.1145/3386569.3392441
12. Y. Ko, J. Kim, S. L. Rodriguez-Zas, J. Kim, *Genes & Genomics* **41**(2) (2019) DOI:10.1007/s13258-019-00789-8
13. I. Karlik, M. Sik, P. Vevoda, T. Skrivan, *ACM Transactions on Graphics* **38**(6), 1-12 (2019) DOI:10.1145/3355089.3356565
14. Y. Liu, K. Xu, L.Q. Yan, *Computer Graphics Forum* **38**(4), 123-133 (2019) DOI:10.1111/cgf.13776
15. S.I. Vyatkin, B.S. Dolgovesov, *Programming and Computer Software* **48**(5), 322–330 (2022) DOI: 10.1134/S0361768822050061
16. S.I. Vyatkin, B.S. Dolgovesov, *IEEE International Multi-Conference on Engineering, Computer and Information Sciences (SIBIRCON)*, 1560-1564 (2022) DOI: 10.1109/SIBIRCON56155.2022.10017079